



OBSERVATIONS OF SUBSTORMS IN APATITY BY MAIN CAMERAS SYSTEM DURING DIFFERENT SPACE WEATHER CONDITIONS

I.V. Despirak¹, V. Guineva², R. Werner²

¹*Polar Geophysical Institute, Apatity, Russia, e-mail: despirak@gmail.com*

²*Space Research and Technology Institute (SRTI), Stara Zagora Department, Bulgaria*

Abstract. We studied the auroras observations during different solar wind conditions by data of the MAIN cameras (Multiscale Aurora Imaging Network) obtained at Apatity (Kola Peninsula, Russia) for two winter seasons: 2014-2015 and 2015-2016. Solar wind and IMF parameters were taken from the OMNI data base. Observations of aurora were conducted in Apatity, magnetic field disturbances were verified by the data of IMAGE magnetometers. All substorms were divided into different groups depending on the space weather conditions. First, the substorms were separated into two groups: substorms observed during storms and substorms under non-storm conditions. The substorms during storms were divided in sub-groups according to observations during different storm phases: initial, main, near and late recovery phases. We considered also specific space weather conditions, when the SYM/H index behavior was highly irregular, we called these conditions "structured recovery phase" of the storm. The non-storm conditions were classified as quiet conditions, when no structures in the solar wind were observed, and as conditions when structures in the solar wind near the Earth were detected, but these structures did not provoke geomagnetic storms. It was shown that the latitude of the substorm onset was controlled by the value of the SYM/H index. It was found out also that the maximal relative intensity of auroras was greater for substorms with onset to the South from Apatity and smaller - for substorms with onset in zenith or to the North from Apatity.

Introduction

Many researchers turned to the problem of studying substorms during geomagnetic storms (e.g. [1]; [2]; [3]; [4]; [5]; [6]; [7]; [8]; [9]). This problem was considered from various angles, using both satellite data (IMAGE, POLAR and others) and ground-based data (IMAGE magnetometers data, AL, AU indexes, data of auroras). It is known that by substorms investigations, it is important to consider whether they were observed during storms or in non-storm periods, and during what phase of the storm they were observed. Typically, initial, main and recovery phases of the storm are specified, while the storm recovery phase is divided into 'near' and 'late', into "rapid" and "recovery" (e.g. [10]). Throughout this paper we will use the terms "near" and "late" recovery phase. It should be noted that many observations indicate also that there are more complicated storm cases, when the magnetic storms are caused by several sources in the solar wind, coming consecutively one after another or partly overlapping, and the storm recovery phase can be of very complicated form ([11]; [12]; [13]; [14]). We will call such storms "storms with structured recovery phase". It has to be stressed that in this work we don't examine the classification of storms by their sources (e.g. CIR-storms, Sheath-, MC- or Ejecta-storms), we confine ourselves just to the examination of storm and non-storm conditions. In more detail, the quantitative categorization of storm phases is given in the section "Data and methods of analysis".

In this work we will consider auroras observations in Apatity using measurements of the camera system MAIN. Apatity is settled at auroral latitudes, its geographic coordinates are 67.58°N, 33.31°E, and the corrected geomagnetic ones – 63.86°N, 112.9°E. As follows from the dynamics of the auroral oval at auroral latitudes different substorm development can be observed. The auroras expansion, registered in Apatity, can consist in movement along different directions according to the location of substorm onset with respect to the location of the observational station (propagation from North to South, from South to North and other directions).

The goal of this work is to review substorm developments during different space weather conditions using measurements of the camera system MAIN in Apatity during two winter seasons: 2014/2015 and 2015/2016.

Data

a) Data used

Measurements from the MAIN in Apatity during 2014-2015 and 2015-2016 seasons have been used. The cameras observational system comprises 4 cameras with different fields of view providing simultaneous observations from spatially separated points ([15]). To study the substorm development data from the Apatity all-sky camera and the Guppy F-044C (GC) camera with field of view ~67° were used. In the all-sky images the central column corresponds to the North-South latitudinal cross section of the auroral zone. These columns from each image within 1-hour interval have been used to construct an all-sky keogram. The GC keograms were built in direction magnetic North (up).

Solar wind and interplanetary magnetic field parameters were taken from the OMNI data base of the CDAWeb. We determined the types of solar wind that can be the drivers of ionospheric disturbances, namely shock waves (IS),

high speed streams from coronal holes (HSS), magnetic clouds (MC) and plasma compression regions in front of these structures (CIR and Sheath) according to [16], [17], [14], [18] and based on the catalog of large-scale solar wind phenomena (<ftp://ftp.iki.rssi.ru/omni/>).

Auroral geomagnetic disturbances were verified by the ground-based data of IMAGE magnetometers network (using the meridional TAR-NAL and MEK-NOR chains and by data of Loparskaya (CGM lat. =65.43°) and Lovozero (CGM lat. = 64.23°) magnetometers. LT values for IMAGE network stations are $LT \approx UT + 1 \div 2$, MLT values for IMAGE network are $MLT \approx UT + 2 \div 3$, for Apatity's MAIN cameras $MLT \approx UT + 3.17$ (~ 3 hours and 10 minutes).

b) Substorm identification

For the substorms selection, we used data of magnetometers and data of all-sky camera. First the presence of a substorm was identified by the IMAGE magnetograms, then the substorm onset at the Apatity's latitude was determined by Sodankylä station (SOD) magnetograms and, if observations in this period were available, additionally, by Loparskaya or Lovozero stations magnetograms. After that we determined the substorm by the data of the MAIN cameras system in Apatity during clear sky measurements. We divided the auroras according to their appearance into 3 groups: to the South from Apatity, to the North from it and near the station zenith, i.e. near the Apatity location (from 0° to ~ ±50° from zenith). It should be emphasized that with these criteria for selecting events, not only isolated substorms are included in the review, but also different intensifications of one substorm. During the examined winter seasons, the all-sky camera registered more than 180 substorms and their intensifications.

c) Observation conditions

First, we divided the conditions of observations into 2 groups: storms (when the minimal SYM/H value $SYM/H_{min} < -50$ nT) and non-storm periods. Second, we divided the observations conditions into sub-groups appropriately to these phases of the storm: initial, main and recovery phases, in the recovery phase also near and late recovery phase were defined. We considered also the events with "structured recovery phase", if after the first, deepest SYM/H minimum, other sizable SYM/H minima were observed. The recovery phase was assumed as structured, if there were SYM/H fluctuations, meeting the condition $(SYM/H_{flmin} - SYM/H_{flmax})/SYM/H_{min} > 0.5$, where the SYM/H_{flmin} is the minimal value reached during the fluctuation and $SYM/H_{flmin} - SYM/H_{flmax}$ represents the amplitude of the fluctuation. The non-storm conditions were classified in two sub-groups regarding the presence of solar wind structures. The first sub-group included events under quiet conditions, when no structures in the solar wind were observed, and the second sub-group included conditions when structures in the solar wind near Earth were present, but these structures did not cause geomagnetic storms.

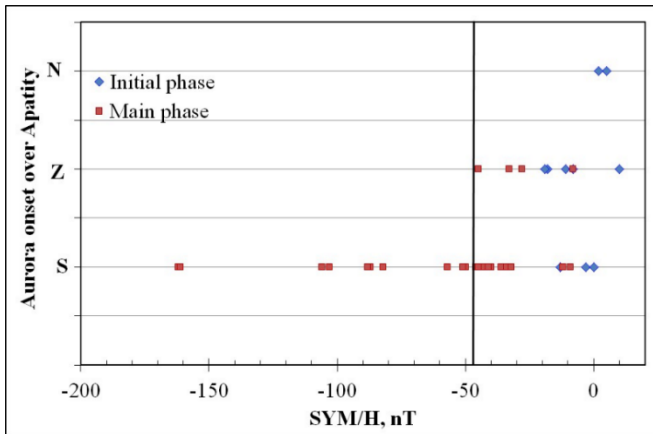


Figure 1. Dependence of the onset location of aurora on SYM/H index. Blue diamonds indicate the events during the initial phase, and red squares – the events during the main phase of the storm.

location (S), to the North from the Apatity (N) and near the station zenith (Z).

In Fig. 1 the dependence of the substorm aurora appearance in Apatity (called further aurora onset over Apatity) on SYM/H index during the initial (blue diamonds) and main (red squares) storm phases is presented. It is seen that at the onset of the geomagnetic storms, during the initial phase, regardless of the higher (often even positive) SYM/H values auroras may originate to the North as well as to the South from Apatity (the blue diamonds in Fig. 1). The black vertical line indicates the boundary between observations of auroras in the South part and in the North part of all-sky camera images. It is seen that at SYM/H values lower from about -45 nT auroras occurred to the South from the station zenith.

Results

In this work we studied the substorms development in Apatity during different space weather conditions. AE and SYM/H geomagnetic indices are the indicators of the geomagnetic activity. We presented here the analysis the location of the onset of auroras depending on the values of AE and SYM/H indices for the different observation conditions (according to the paragraph "c" from the section "data"). It should be noted that we have not found significant differences between the different groups of auroras onset during different observations conditions depending on AE index (this picture is not presented here). The results for the dependence of the aurora locations on the SYM/H index values for the different groups of space weather conditions are presented in Figs. 1, 2 and 3. After their appearance auroras were divided into 3 groups according to the location of the initial auroras: to the South from the Apatity

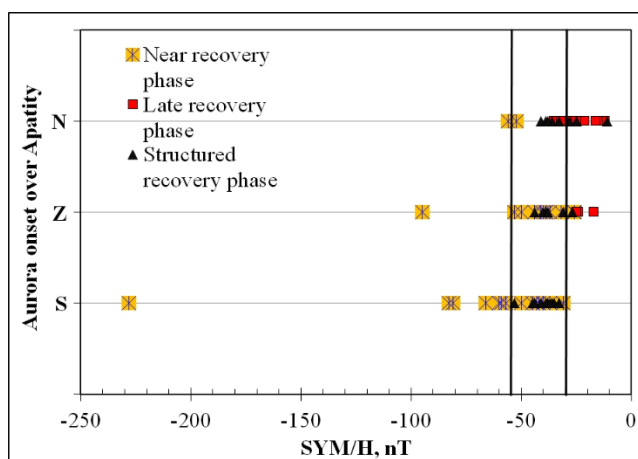


Figure 2. Dependence of the onset location of aurora on SYM/H index. The events during the near, late and structured storm recovery phase are marked by yellow, red squares and black triangles, respectively.

The dependence of the aurora onset on SYM/H index for substorms during the recovery phase of geomagnetic storms is shown in Fig. 2. It is seen that the events during the near recovery phase (the yellow squares in Fig. 2) occurred mainly near the station zenith or to the South from it. The events during the late recovery phase were observed mainly to the North from Apatity. During the structured recovery phase the auroras originated to South or North from Apatity depending on the SYM/H index values. In generally auroras at higher values of SYM/H are observed to the North from Apatity, and auroras movement from North to South is observed. Substorms at lower SYM/H values originate to the South of Apatity and the aurora propagation from South to North can be seen. Between these two types of substorms a “border” zone is formed in which aurora onset can become to the South, over zenith or to the North regarding the station. This zone is in the range from -30 nT to about -55 nT, and it is designated by black vertical lines in Fig. 2.

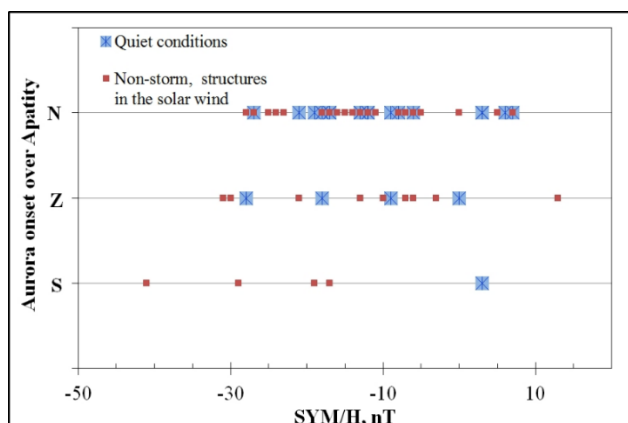


Figure 3. Dependence of the onset location of aurora on SYM/H index. The events during quiet conditions and during non-storm conditions with solar wind structures are marked by blue and red squares, respectively.

Fig. 3 shows the dependence of the aurora onset on SYM/H index for events during non-storm conditions. It is seen that no evident dependence of the aurora onset on SYM/H values during non-storm conditions is obtained. Auroras during quiet conditions appeared mostly to the North from zenith or near zenith, and auroras during non-storm conditions with some solar wind structure occurred at different positions – to the North, near zenith or to the South from Apatity.

Discussion

In this paper we investigated the location of onset latitude of substorms during storm and non-storm conditions using observations of auroras in Apatity during two winter observational seasons 2014-15 and 2015-16. The most significant result is that the latitude of the substorm onset is controlled by the value of the SYM/H index. This result is in good agreement with the findings of *Milan et al.* [4]. In particular, one of the main conclusions in this work was that the open flux content of the magnetosphere increased dramatically and substorms became more intense during geomagnetic storm activity, when the SYM/H index was depressed. It has to be mentioned, that in papers [4], [5] the substorm onset latitude was used as a measure of the polar cap size. If the substorm onset latitude decreases, the polar cap is expanded and the open magnetic flux is increased. It turns out that the results found out in the present paper are very similar.

As a whole, our work by new ground-based data holds the findings of paper [5], that when studying substorms during geomagnetic storms it is necessary to consider both: the solar wind-magnetosphere coupling and the ring current intensity, and that it is better to examine the influence of these factors not individually, but together.

Conclusions

- Substorms during the initial storm phase or at higher SYM/H values during the main storm phase can appear to North or South regarding the station zenith. Substorms during the main phase at SYM/H values lower than about -45 nT are observed to the South from Apatity (64.27°N CGM Lat.) and auroras expansion in North direction is seen.
- Substorms during the near recovery phase originated mainly near the station zenith or to the South from Apatity, and auroras expansion to North was observed.
- For substorms during the late recovery phase or under quiet conditions, auroras were observed near the station zenith or to the North of the Apatity station, and their motion from North to South was registered.
- For substorms during a structured storm recovery phase or during “non-storm conditions with structures in the solar wind” auroras may occur first to the South or to the North from the station zenith.

Thus, substorms at higher values of SYM/H index occur to the North from station zenith, and at smaller SYM/H values – to the South of it. The boundary between both types of substorms in terms of SYM/H index is in the range from ~-30 nT to about -55 nT.

Acknowledgments. We express our gratitude to Dr. B.V. Kozelov for the possibility of using the data of the observational cameras in Apatity, the construction of keograms and the useful discussions. The paper was supported partly by Program No 7 of the of the Presidium of RAS. The study is also a part of a joint Russian - Bulgarian Project 1.2.10 of PGI RAS and IKIT-BAS under the Fundamental Space Research Program between RAS and BAS.

References

1. Hsu T.-S., McPherron R.L. (2000) The characteristics of storm-time substorms and non-storm substorms. Proc. of Fifth International Conference on Substorms, 16-20 May, 2000, St. Petersburg, Russia. Edited by A. Wilson. ISBN: 92-9092-772-0., 439.
2. Tsurutani B.T., Gonzales W.D., Guarnieri F., Kamide Y., Zhou X., Arballo J.K. (2004) Are high-intensity long-duration continuous AE activity (HILDCAA) events substorm expansion events? *J. Atmos. Solar-Terr. Phys.* 66, 167–176.
3. Wu C.-C., K. Liou K., Lepping R.P., Meng C.-I. (2004) Identification of substorms within storms. *J. Atmos. Solar-Terr. Phys.* 66, 125–132.
4. Milan S.E., Boakes P.D., Hubert B. (2008). Response of the expanding/contracting polar cap to weak and strong solar wind driving: Implications for substorm onset. *J. Geophys. Res.* 113, A09215, doi:10.1029/2008JA013340.
5. Milan S.E., Grocott A., Forsyth C., Imber S.M., Boakes P.D., Hubert B. (2009) A superposed epoch analysis of auroral evolution during substorm growth, onset and recovery: open magnetic flux control of substorm intensity. *Ann. Geophys.* 27, 659–668.
6. Hoffmann R.A., Gjerloev J.W., Frank L.A., Sigwarth J.W. (2010) Are there optical differences between storm-time substorms and isolated substorms? *Ann. Geophys.* 28, 1183-1198. doi:10.5194/angeo-28-1183-2010.
7. Partamies N., Jussola L., Tanskanen E., Kauristie K., Weygand J.M., Ogawa Y. (2011) Substorms during different storm phases. *Ann. Geophys.* 29, 2031–2043.
8. Despirak I.V., Lubchich A.A., Yahnin A.G., Kozelov B.V., Biernat H.K. (2009) Development of substorm bulges during different solar wind structures. *Ann. Geophys.* 27, 1951-1960.
9. Despirak I.V., Lubchich A.A., Guineva V. (2011) Development of substorm bulges during storms of different interplanetary origins. *J. Atmos. Solar-Terr. Phys.* 73, 1460–1464.
10. Terada N., Iyemori T., Nosé M., Nagai T., Matsumoto H., Goka T. (1998) Storm-time magnetic field variations observed by the ETS-VI satellite. *Earth Planets Space.* 50, 853–864.
11. Huttunen K.E.J., Koskinen H.E.J., Karinen A., Mursula K. (2006) Asymmetric development of magnetospheric storms during magnetic clouds and sheath regions. *Geophys. Res. Lett.* 33(6), L06107, DOI: 10.1029/2005GL024894.
12. Pulkkinen T.I., Ganushkina N.Y., Tanskanen E.I., Kubyshkina M., Reeves G.D., Thomsen M.F., Russel C.T., Singer H.J., Slavin J.A., Gjerloev J. (2006). Magnetospheric current systems during stormtime sawtooth events. *J. Geophys. Res.* 111, A11S17, DOI: 10.1029/2006JA011627.
13. Yermolaev Yu.I., M.Yu. Yermolaev (2006), Statistic study on the geomagnetic storm effectiveness of solar and interplanetary events. *Adv. Space Res.* 37, 11 75-1181.
14. Tsurutani B.T., Echer E., Shibata K., Verkhoglyadova O.P., Mannucci A.J., Gonzalez W.D., Kozyra J.U., Pätzold M. (2014). The interplanetary causes of geomagnetic activity during the 7-17 March 2012 interval: a CAWSES II overview. *J. Space Weather and Space Climate.* 4, A02, DOI: 10.1051/swsc/2013056.
15. Kozelov B.V., Pilgaev S.V., Borovkov L.P., Yurov V.E. (2012). Multi-scale auroral observations in Apatity: winter 2010-2011. *Geoscientific Instrumentation, Methods and Data Systems.* 1(1), 1-6.
16. Balogh A., Gosling J.T., Jokipii J.R., Kallenbach R., Kunow H. (1999) *Space Sci. Rev.* 89, 141.
17. Burlaga L.F., Klein L., Sheeley N.R., Michels Jr., Howard D.J., Koomen R.A., Schwenn M.J., Rosenbauer H. (1982) *Geophys. Res. Lett.* 9, 1317.
18. Yermolaev Yu.I., Nikolaeva N.S., Lodkina I.G., Yermolaev M.Yu. (2009) Catalog of Large-Scale Solar Wind Phenomena during 1976–2000. *Cosmic Research (Engl. Transl.)*, 47, 81-94.